Sea Ice Suppression of CO₂ Outgassing in the West Antarctic Peninsula: Implications For The Evolving Southern Ocean Carbon Sink

E. H. Shadwick[1,2,3] , O. A. De Meo[4], S. Schroeter[1] , M. C. Arroyo[4] , D. G. Martinson[5] , and H. Ducklow[5]

[1]CSIRO Oceans & Atmosphere, Hobart, TAS, Australia, [2]Australian Antarctic Program Partnership, Institute for Marine and Antarctic Studies, University of Tasmania, Hobart, TAS, Australia, [3]Centre for Southern Hemisphere Oceans Research, Hobart, TAS, Australia, [4]Virginia Institute of Marine Science, College of William & Mary, Gloucester Point, VA, USA, [5]Lamont-Doherty Earth Observatory, Columbia University, Palisades, NY, USA

Abstract The Southern Ocean plays an important role in the uptake of atmospheric CO₂. In seasonally ice-covered regions, estimates of air-sea exchange remain uncertain in part because of a lack of observations outside the summer season. Here we present new estimates of air-sea CO₂ flux in the West Antarctic Peninsula (WAP) from an autonomous mooring on the continental shelf. In summer, the WAP is a sink for atmospheric CO₂ followed by a slow return to atmospheric equilibrium in autumn and winter. Outgassing is almost entirely suppressed by ice cover from June through October, resulting in a modest net annual CO₂ sink. Model projections indicate sea ice formation will occur later in the season in the coming decades potentially weakening the net oceanic CO₂ sink. Interannual variability in the WAP is significant, highlighting the importance of sustained observations of air-sea exchange in this rapidly changing region of the Southern Ocean.

Plain Language Summary The Southern Ocean absorbs a considerable amount of carbon dioxide from the atmosphere and plays an important role in regulating climate on Earth. Ice covered regions of the Southern Ocean are difficult to access and observations are often limited to the ice-free summer season. Here we present new observations over a full 12 month period from a mooring on the continental shelf of the West Antarctic Peninsula (WAP). The observations indicate that the WAP absorbs carbon dioxide in the summer season, while the presence of sea ice in winter prevents that carbon from being released back to the atmosphere. Over the next few decades less sea ice is expected to form and this may lead to a weakening of the carbon dioxide uptake in the WAP region.

1. Introduction

The Southern Ocean is the central connecting feature that links the major ocean basins of the world, playing a crucial role in the global carbon cycle. Present-day Southern Ocean carbon fluxes reflect both significant uptake of anthropogenic CO₂ emissions (Frolicher et al., 2015; Khatiwala et al., 2013; Sabine et al., 2004) and spatial variations in the balance between uptake and release of natural CO₂ (Lenton et al., 2012, 2013; Metzl et al., 2006; Takahashi et al., 2009). Despite the importance of the region to the global climate, major uncertainties persist in our understanding of the Southern Ocean carbon budget (e.g., Gruber et al., 2009), due in part to unresolved variability at the seasonal time scale, and strong disagreement among simulated seasonal cycles in global carbon models (Lenton et al., 2013; Resplandy et al., 2015).

A wealth of continuous surface water CO₂ partial pressure (pCO₂) data has been collected in the Southern Ocean by resupply ships for the various Antarctic stations and on scientific vessels, and these data have been used to constrain the air-sea flux of CO₂ (Bakker et al., 2016; Fay et al., 2018; Landschutzer et al., 2013; Munro, Lovenduski, Stephens, et al., 2015; Takahashi et al., 2014). Recently, the open water bias in the shipboard data has been addressed using observations from biogeochemical floats (Bushinsksy et al., 2019; Gray et al., 2018; Williams et al., 2017, 2018).

A suite of environmental drivers representing important feedbacks to the carbonate system complicates the assessment of changing chemistry in Antarctic coastal regions. Warming, freshening (due to an increased
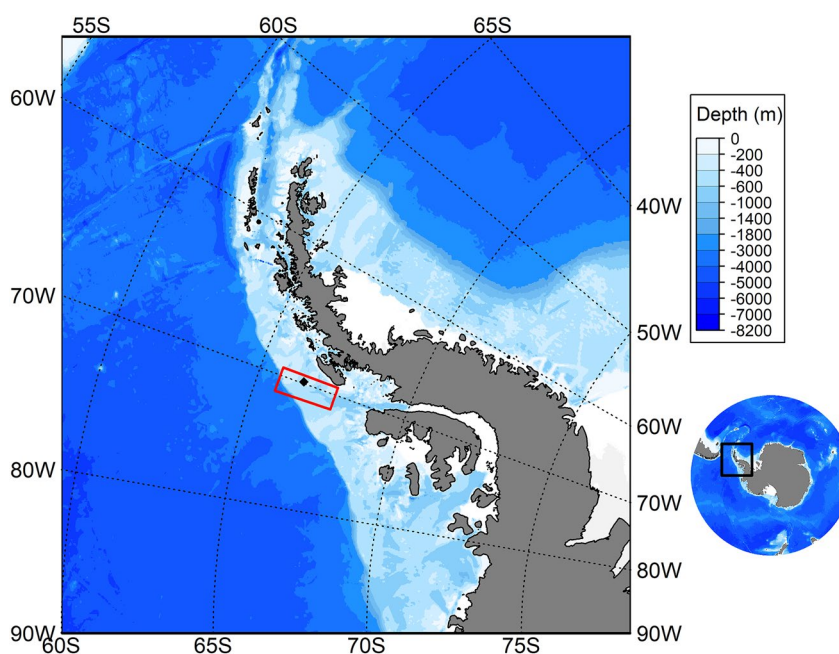
Figure 1. Location of the mooring (black square) in the West Antarctic Peninsula. The red box indicates the region in which sea ice cover and wind speed data were obtained to compute the air-sea CO_2 fluxes.

input of both sea-ice and glacial melt-water; Meredith et al., 2016), enhanced biological productivity (potentially due to a longer open water season, enhanced upper ocean stability and/or increased delivery of nutrients; e.g., Moreau et al., 2015), and intrusions of carbon-rich upper circumpolar deep water onto the continental shelf may influence carbonate system seasonality in ways that may exacerbate or mask the pervasive trend of increasing atmospheric CO_2.

While there are a few nearshore locations where annual cycles have been resolved with sampling from Antarctic stations (Gibson & Trull, 1999; Legge et al., 2015, 2017; Roden et al., 2013), the seasonally ice-covered regions of the Southern Ocean remain poorly sampled, with a large portion of this region comprised of relatively shallow shelves beyond the reach of profiling floats. The West Antarctic Peninsula (WAP) continental shelf is roughly 200 km wide and has an average depth of 430 m (Figure 1). Studies have shown that the climatological southern boundary of the Antarctic Circumpolar Current (ACC) lies along the continental shelf in the WAP region (Orsi et al., 1995; Martinson et al., 2008). Because of the proximity of the ACC to the continental shelf, incursions of upper circumpolar deep water (uCDW) consistently move onto the WAP shelf at the northern end of Marguerite Trough, a large cross-shelf channel. These onshore intrusions of uCDW are consistent with the circulation and dynamic topography, and the shelf bathymetry has been identified as a key mechanism for delivering uCDW onto the shelf (Martinson et al., 2008).

The WAP has experienced some of the largest changes in atmospheric temperature (more than 0.5°C per decade), which have been accompanied by a shortened sea ice season (e.g., Massom & Stammerjohn, 2010; Stammerjohn et al., 2008) and the progressive transition from a polar to subpolar climate (Smith et al., 2003). Recent work indicates that the decrease in duration of winter sea ice extent is due to both later sea ice advance and earlier sea ice retreat (Massom & Stammerjohn, 2010; Stammerjohn et al., 2008); these environmental changes are associated with shifts in phytoplankton community structure (Montes-Hugo et al., 2009; Moreau et al., 2015), and potentially in the carbonate system given the strong influence of summertime primary production on mixed layer inorganic carbon (Brown et al., 2019; Carillo & Karl, 1999; Carillo et al., 2004; Legge et al., 2017; Moline et al., 2008; Yang et al., 2021).

Increases in annually-averaged chlorophyll concentrations (i.e., primary production) in the WAP due to a longer open water season are expected (Montes-Hugo et al., 2009; Moreau et al., 2015), but the impact of this change on the CO_2 system in other seasons, when observations are sparse, is not known. An analysis of summertime data from the Palmer Long-Term Ecological Research (PAL-LTER) voyages, indicates that

there is no long-term trend in summer surface pCO_2 in the Central WAP (Hauri et al., 2015), while in the northern region of the WAP, summer surface pCO_2 appears to be changing more slowly than the global mean (Munro, Lovenduski, Takahashi, et al., 2015). Recently, Brown et al. (2019) showed a strong link between upper ocean stability and the summer season uptake of atmospheric CO_2, but suggest that ongoing ice loss and warming may result in decreased primary production, weakening the open water sink for CO_2.

Here we present air-sea CO_2 fluxes over a full annual cycle from mooring observations on the WAP continental shelf, a region undergoing significant environmental change, including a shortening of the sea ice season. We compare the seasonality in air-sea CO_2 fluxes to those computed from profiling floats in the seasonal ice zone and examine the implications of changing sea ice cover from Coupled Model Intercomparison Project Phase 6 (CMIP6, Eyring et al., 2016) projections on the uptake of atmospheric CO_2 in the shelf waters of the WAP.

2. Methods

2.1. Mooring Observations

A mooring was deployed at station 300.100 on the PAL-LTER grid (latitude: 66.5°S, longitude: 69.9°W) in water roughly 480 m deep on the WAP continental shelf (Figure 1). The mooring was based on the design used for physical oceanographic monitoring described by Martinson and McKee (2012), with additional biogeochemical sensors in the upper water column (at 12–15 m depth—see Supporting Information for additional detail about deployed sensors and their calibration; Figures S1 and S2); this analysis is focused on daily averaged data from the period January to December, 2018 (Shadwick & De Meo, 2020).

2.2. Mixed-Layer Depth Computation

The mixed layer depth (MLD) was determined following Weeding and Trull (2014) using a series of temperature sensors deployed along the mooring line. Temperatures were collected at roughly 12, 17, 25, 34, 42, 50, 58, 66, 74, 90 and 110 m and interpolated vertically to 1 m resolution to a daily resolution and MLD was computed using a threshold of 0.2°C from the 10 m value. While it is possible that stratification in summer due to meltwater input may result in mixed layers shallower than the uppermost sensor, these conditions are not generally observed on the shelf (e.g., Meredith et al., 2016), and we therefore assume that the shallowest sensors are representative of the near surface conditions (see Figure S3 for seasonal profiles of temperature from the mooring).

2.3. Air-Sea CO_2 Flux Computations

The air-sea CO_2 flux at the mooring location was computed according to $F = k\alpha\Delta pCO_2$, where k and α are the gas transfer velocity, and the coefficient of solubility (Weiss, 1974), respectively, ΔpCO_2 is the pCO_2 of the ocean minus that of the atmosphere, and a negative flux indicates an ocean uptake. The oceanic pCO_2 was computed from pH and alkalinity (e.g., Gray et al., 2018; Williams et al., 2017 see Supplementary Information). Atmospheric pCO_2 was computed from the dry mole fraction (xCO_2) from Palmer Station collected by National Oceanic and Atmospheric Administration (NOAA) Earth System Research Laboratories. The gas transfer velocity was computed using the formulation of Wanninkhof (2014) with daily-averaged winds at 10 m above the sea surface (U_{10}) from the NCEP/NCARR Reanalysis product (Kalnay et al., 1996). As noted above, it is possible that water column stratification develops above the depth of the moored sensors in the summer season, when biological activity is at a maximum. This would result in an overestimate in the observed pCO_2, and an underestimate in the air-sea gradient, and correspondingly the air-sea CO_2 flux under those conditions.

The fluxes were scaled linearly for the presence of sea ice by multiplying the gas transfer velocity by the fraction of open water (Butterworth & Miller, 2016). Sea ice concentrations in a region around the mooring location (Figure 1 and Figure S4) were obtained from Special Sensor Microwave/Imager (SMM/I) and the Special Sensor Microwave Imager/Sounder (SMMIS) on the Defense Meteorological Satellite Program (DMSP) satellite from the National Snow and Ice Data Center (NSIDC, see Figure S4). The air-sea CO_2 fluxes have associated uncertainty from a number of sources, which are discussed in detail in the Supporting

Information. We note that this uncertainty is particularly important during periods when the air-sea gradients are weak as uncertainty in the flux computations may impact the determination of source/sink status of the region.

2.4. Projections of Sea Ice Seasonality

The CMIP6 is a coordinated, standardized suite of state-of-the-art global climate model experiments, including control scenarios (unforced pre-industrial conditions spanning several centuries), forced "historical" scenarios spanning 1850–2014, and scenario-based future climate projections (Eyring et al., 2016; O'Neill et al., 2016). This tool allows observational datasets, such as those presented here, to be evaluated in the context of anticipated future environmental change. Using models in which sea ice concentration (SIC) data was available from all three experiments, climatologies and historical trends were compared to the NOAA NSIDC Climate Data Record, of SIC from passive microwave data (Meier et al., 2017; Peng et al., 2013). Individual model members with monthly sea ice concentration data from both the historical and the middle-of-the-road Shared Socioeconomic Pathways (SSP2) experiments were concatenated, and trends calculated for multiple future project periods via a linear least-squares regression (see Figure S5).

3. Results and Discussion

3.1. Annual Cycles

The annual cycles of sea ice cover and mixed layer temperature from the 2018 deployment are shown in Figures 2a and 2b. The WAP is ice-free from January to late June. After the onset of sea ice formation, the region changed rapidly, with ice cover nearing 100% after only a few weeks in July. The WAP continental shelf remained nearly completely ice covered until late October when a more gradual ice melt led to <50% open water area by late November, and ice-free conditions in December. We note that the 2018 year had relatively more complete cover (e.g., greater %SIC) than recent years (see Figure S4). Observations between 2015 and 2020 indicate significant variability in ice cover through the autumn and winter seasons. In some years 100% ice cover is not observed and concentrations vary by $\sim 20\%$ throughout the period.

The seasonality in temperature is similarly stark, with open water, summer temperatures exceeding 2°C between January and mid-March. The temperature begins to fall in April, before the onset of sea-ice, and remains very stable at -1.8°C between mid-June and early November, coincident with the presence of sea ice. The waters begin to warm in mid-November through the end of the year.

The summer mixed layer depth is between ~ 20 and 40 m and is relatively stable through the open water season (Figure 2c). The mixed layer begins to deepen in late March and reaches a maximum of 100 m during the period of observation, with variability on weekly and shorter timescales, though never shoaling above 60 m throughout the ice-covered winter season, and generally remaining deeper than 80 meters between July and November.

The seasonal cycle in total dissolved inorganic carbon (TCO_2, Figure 2d) is influenced by biological processes, air-sea exchange of CO_2 and physical processes, including the upward mixing of TCO_2-rich subsurface waters. Biology is the dominant driver of the seasonal decrease in TCO_2, which begins in mid-November, coincident with the retreat of sea ice and the relief of light limitation for phytoplankton (Smith et al., 2008). Outgassing of CO_2 also contributes to this decrease as the waters are supersaturated at the onset of sea ice retreat (Figure 2e). A summer phytoplankton bloom results in minimum seasonal TCO_2 concentrations at the end of the time series; this surface depletion appears to be short-lived, with increases beginning as the water temperature declines and the mixed layer deepens, indicating an entrainment of TCO_2-rich subsurface waters into the mixed layer and a likely contribution from respiration of organic matter produced in the open water season (Yang et al., 2021). The winter TCO_2 concentrations are fairly stable under the cover of sea ice.

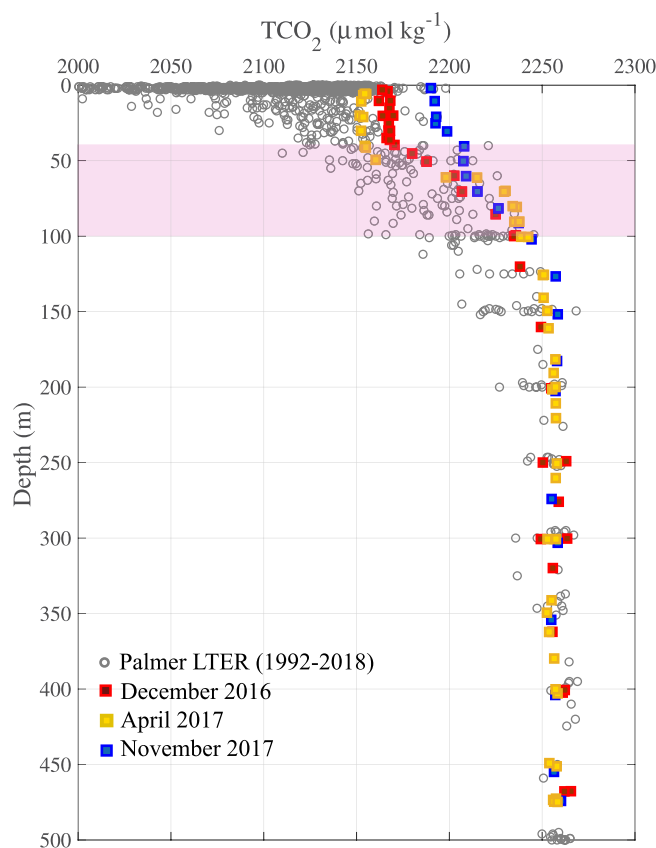Profiles of TCO_2 at the mooring location and in the broader WAP region (Figure 3 and Supporting Information) reinforce the seasonal changes in TCO_2 and their drivers described above. In particular, subsurface concentrations (at depths between 50 and 100 m) directly below the mixed layer are up to 100 μmol kg^{-1} higher than surface values; a deepening of the mixed layer results in increased surface TCO_2. The maximum
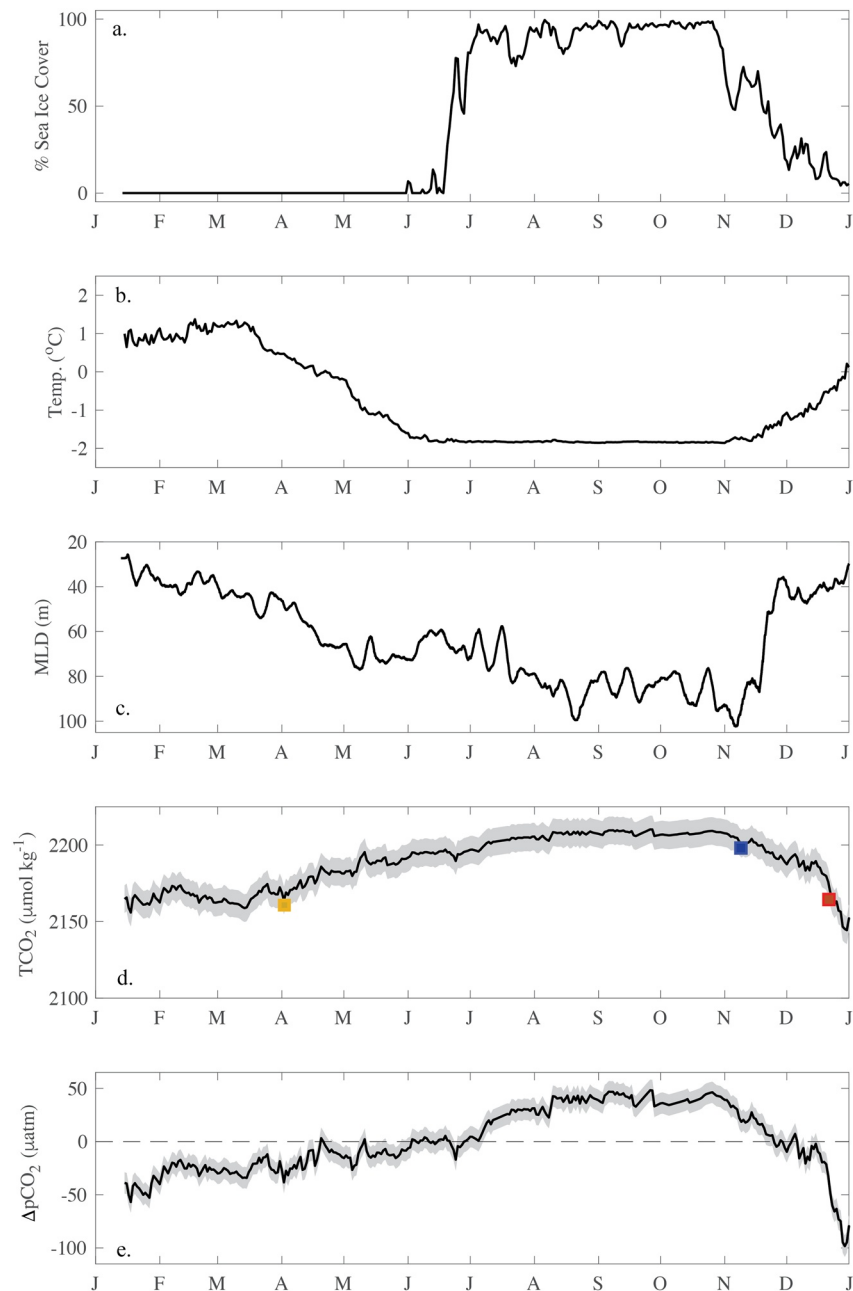
Figure 2. Seasonal cycles of: (a) Percentage sea ice cover, (b) temperature, (c) mixed-layer depth, (d) TCO_2 and (e) ΔpCO_2 collected at ~15 m below the surface from January 2018 to January 2019. The colored squares in panel d correspond to discrete samples collected at the mooring location in December 2016 (red), April 2017 (yellow), and November 2017 (blue); the shading in panels d and e indicates the uncertainty associated with the derived TCO_2 and ΔpCO_2 (see Supporting Information).

surface TCO_2 concentration is observed in November and is associated with the remineralization of organic matter. The surface TCO_2 decline begins in December coincident with the onset of the productive season. The seasonal minimum occurs fairly late in the season, represented here by the autumn profile obtained in April. We note that while the majority of these ship-based profiles were not collected in the same year as the mooring was deployed, they nevertheless broadly reflect seasonality in TCO_2 inferred from the moored sensors.

Figure 3. Profiles of TCO_2 at the mooring location and in the broader Wester Antarctic Peninsula region. The long-term observations (1992–2018) samples from the Palmer LTER are shown in gray, while samples collected at the mooring location are shown in red (December 2016), yellow (April 2017), and blue (November 2017). The pink shaded area indicates the computed range of mixed layer depth throughout the 2018 deployment (see also Figure 1c).

The seasonality in TCO_2 is also reflected in the gradient of CO_2 partial pressure between the surface ocean and the atmosphere in the WAP (ΔpCO_2, Figure 2e). The surface waters are undersaturated during the ice-free summer season, with air-sea disequilibrium reaching a maximum of 100 µatm in late December. Re-equilibration with the atmosphere is coincident with the deepening of the mixed layer, reinforcing the importance of the delivery of subsurface water in increasing the surface water pCO_2, in addition to the contribution from remineralization as discussed above. The WAP transitions from a sink for atmospheric CO_2 to a source in early July, at which point the region is nearly 100% ice covered; the implications of this timing will be explored in more detail below. The winter season supersaturation under the ice is a relatively constant 50 µatm between August and November, and begins to decline with the onset of sea ice melt and biological activity as TCO_2 is converted to organic matter by phytoplankton as described above.

3.2. Air-Sea CO_2 Exchange in the West Antarctic Peninsula

The air-sea CO_2 flux, computed with a linear scaling for ice cover (Figure 4) indicates that the WAP acts as a weak sink for atmospheric CO_2 in the spring and summer seasons, and transitions to a weak source of atmospheric CO_2 during the ice-covered autumn and winter. While the direction of the flux is determined by the air-sea gradient (Figure 2e), the magnitude is also determined by the wind speed, and in this case, strongly mediated by the degree of ice cover. The transition from uptake (negative flux) to outgassing (positive flux) is remarkably coincident with the onset of ice cover (Figure 4). The subsequent transition from outgassing to uptake is also associated with the ice retreat, as has previously been reported in polar systems (e.g., Roden et al., 2013; Shadwick et al., 2011) and is strongly linked to the relief of light limitation and the onset of biological productivity, likely commencing under the ice and continuing in the open water.

Also shown in Figure 4 are the fluxes that have not been scaled for ice cover. Note that we are not suggesting that the linear scaling for ice cover is inappropriate, or that the sea ice did not impose some barrier to atmospheric exchange. Rather, we use the unscaled fluxes to assess the seasonality of factors controlling the magnitude of CO_2 uptake in the WAP, and to inform a discussion of future changes in the region in the following sections.

We first consider the seasonality of the air-sea CO_2 flux in the WAP compared to observations obtained using biogeochemical floats. The annual cycle of air-sea flux constructed from biogeochemical float data in the Seasonal Ice Zone by Gray et al. (2018) indicates the same stark transition from summer (DJF) sink to source, but this transition occurs much earlier in the float data, at the beginning of April, approximately three months before the onset of sea ice formation. While the air-sea fluxes of Gray et al. (2018) are similarly scaled for the presence of ice cover, they observed a sizable outgassing in autumn before the return of sea ice (Gray et al., 2018 their Figure 2).

In the WAP, the re-equilibration with the atmosphere is slower, such that the transition from sink to source occurs only when the region is nearly completely ice covered, and if the conventional linear scaling is applied, the sea ice acts to nearly completely suppress outgassing in the region. Observations of ice cover in the vicinity of the mooring indicate substantial leads in the winter season (e.g., Figure S3), which may potentially have been associated with enhanced air-sea exchange (e.g., Loose et al., 2009). We note that the magnitude of the outgassing in the WAP (when not scaled for ice cover) is similar to what was obtained with the floats, but the timing occurs much later in mid-winter, and under the ice. This results in very different assessments of the magnitude of net flux over the year: -0.5 ± 1.0 mol C m^{-2} yr^{-1} in the WAP versus
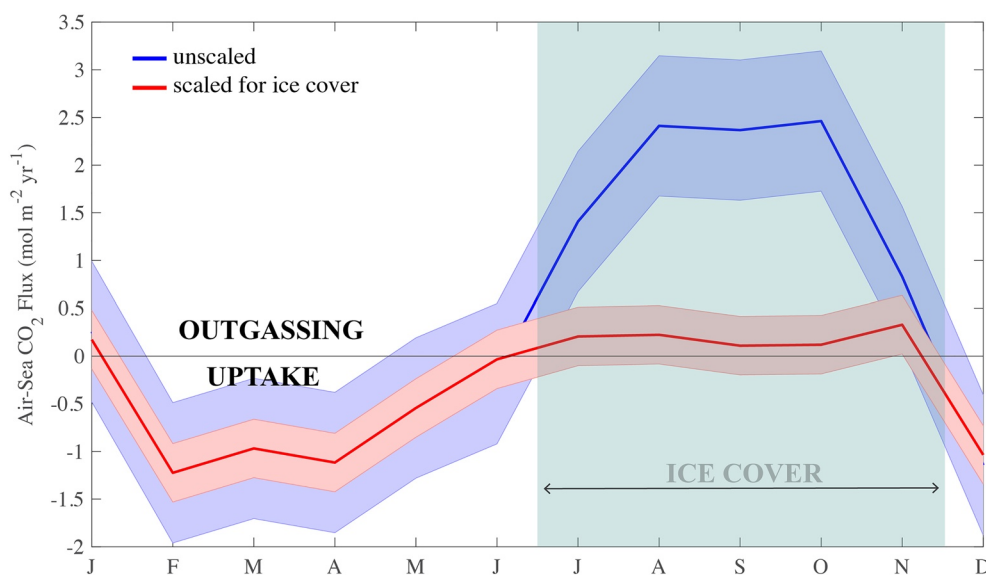
Figure 4. Annual air-sea CO_2 flux in the Western Antarctic Peninsula with (red) and without (blue) scaling for sea ice cover; shaded areas around the lines indicate the standard deviation of the monthly mean values. The period of ice cover is shown schematically by the blue box.

-0.04 ± 0.31 mol C m^{-2} yr^{-1} in the seasonal ice zone (SIZ) from Gray et al., 2018, though the two datasets agree on the sign of the flux indicating uptake by the ocean. We note as well that the observations of Gray et al.,2018 represent a combination of data from the Bellingshausen and Weddell Sea regions, and may be more representative of the broader seasonally ice-covered Southern Ocean, whereas the WAP is often considered somewhat subpolar with respect to its physical and biogeochemical properties (e.g., Shadwick et al., 2013).

A reduction in sea ice may be expected to weaken the Southern Ocean oceanic CO_2 sink, by allowing additional outgassing in autumn and winter when the surface waters are supersaturated as a result of both local biological processes and the introduction of carbon-rich water from the subsurface. The latter process is linked reduced sea ice cover as greater areas of open water are associated with greater wind-driven mixing, resulting in enhanced delivery of water from below. There is an additional feedback, as enhanced winter mixing may lead to weaker stratification in summer (e.g., Venables & Meredith, 2014), resulting in a less stable mixed layer, weaker relief of light limitation, and suppressed biological production, associated with smaller seasonal drawdown of CO_2.

To evaluate the impact of the expected continuation of sea ice decline in the WAP on the oceanic sink for CO_2 in the region, we turn to projections of sea ice climatology (i.e., the mean seasonal cycle) and the expected trends in sea ice coverage over the coming decades from a suite of CMIP6 simulations (see Figure S5). The available models, from a range of international modeling institutes and encompassing a wide array of individual model components, have a large spread in mean sea ice in the region of the mooring site; however, over the historical period (1979–2019), many models show varying degrees of delayed onset of sea ice advance. The models that most closely match the curve of the observed historical trend during advance generally agree that in the short term, SIC will decline from approximately May through to the sea ice maximum and, toward the end of the century, the majority also suggest declines into the season of sea ice retreat, thus shortening the period of continuous ice cover from either or both ends (Figure S4).

If we assume that the mooring observations obtained here represent the expected seasonality of air-sea exchange in the coming decades, this trend suggests important implications for the CO_2 sink in the region. At present, biological activity results in a relatively strong (on the order of 100 µatm) undersaturation of the surface waters in the WAP. While the biological activity appears to be restricted to a brief period of open water productivity, the return to atmospheric equilibrium takes several months, and is currently achieved under the cover of sea ice. If the timing of the sea ice advance occurs later, as the model projections suggest,

the region is likely to exhibit outgassing in advance of the winter season. This change in timing may also impact the degree of CO_2 supersaturation directly, by enhancing wind-driven mixing and subsequently the supply of CO_2-rich subsurface water. Both the later sea ice advance and the enhanced mixing may weaken the oceanic CO_2 sink in this region.

On the other side of the seasonal cycle, a decline in sea ice cover during the period of sea ice retreat (between September and December), may also result in enhanced outgassing, as the current seasonality suggests that the biologically driven undersaturation is not achieved until November when the system returns to net autotrophic (i.e., photosynthesis > respiration) conditions. We note that there is potential to offset some of this late season outgassing with enhanced biological productivity in the subsequent open water season fueled by unused nutrients supplied by enhanced mixing in ice free waters in the autumn season, and potentially also a longer growing season with earlier sea ice retreat. However, both the spring and autumn seasons will remain light limited in this high latitude region independent of changes to ice cover, thereby restricting the potential offset of outgassing by additional biological production.

4. Conclusions

It has been suggested that Antarctic coastal regions may be less vulnerable than their Arctic counterparts with respect to expected increases in pCO_2, and decreases in pH resulting from increased atmospheric and thus oceanic CO_2 concentrations (Shadwick et al., 2013). This is due both to the enhanced alkalinity (relative to Arctic Ocean waters), and the potential for biological activity to offset the increase in pCO_2. A full seasonal cycle of air-sea CO_2 fluxes from the WAP, and its connection to observed cycles of sea ice cover and biological productivity presented here, albeit from a single mooring location, suggests that the region will experience increased CO_2 outgassing with anticipated changes to sea ice cover in the coming decades. This is likely despite potentially greater uptake due to enhanced biological production in the summer season, assuming sufficient nutrients are available. In addition, at the end of open water season, upward mixing of CO_2-rich subsurface water is likely to accelerate the re-equilibration with the atmosphere, and may lead to an overall weakening of the WAP CO_2 sink.

Data Availability Statement

Mooring data are available through William & Mary's Scholarworks program (https://doi.org10.25773/0nxb-wm54).

References

Bakker, D. C. E., Pfeil, B., Landa, C. S., Metzl, N., O'Brien, K. M., Olsen, A., et al. (2016). A multi-decade record of high-quality *f*CO₂ data in version 3 of the Surface Ocean CO₂ Atlas (SOCAT). *Earth System Science Data*, *8*(2), 383–413. https://doi.org/10.5194/essd-8-383-2016,2016

Bresnahan, P. J., Martz, T. R., Takeshita, Y., Johnson, K. S., & LaShomb, M. (2014). Best practices for autonomous measurement of seawater pH with the Honeywell Durafet. *Methods in Oceanography*, *9*, 44–60. https://doi.org/10.1016/j.mio.2014.08.003

Brown, M. S., Munro, D. R., Feehan, C. J., Sweeney, C., Ducklow, H. W., & Schofield, O. M. (2019). Enhanced oceanic CO₂ uptake along the rapidly changing West Antarctic Peninsula. *Nature Climate Change*, *9*, 678–683. https://doi.org/10.1038/s41558-019-0552-3

Bushinksky, S. M., Landschutzer, P., Rodenbeck, C., Gray, A. R., Baker, D., Mazloff, M. R., & Sarmiento, J. L. (2019). Reassessing Southern Ocean air-sea CO₂ flux estimates with the addition of biogeochemical float observations. *Global Biogeochemical Cycles*, *33*(11), 1370–1388. https://doi.org/10.1029/2019GB006176

Butterworth, B. J., & Miller, S. D. (2016). Automated underway eddy covariance system for air-sea momentum, heat, and CO₂ fluxes in the Southern Ocean. *Journal of Atmospheric and Oceanic Technology*, *33*(4), 635–652. https://doi.org/10.1175/jtech-d-15-0156.1

Carillo, C. J., & Karl, D. M. (1999). Dissolved inorganic carbon pool dynamics in northern Gerlache Strait, Antarctica. *Journal of Geophysical Research*: Oceans, *104*(C7), 15,873-15,884. https://doi.org/10.1029/1999jc900110

Carillo, C. J., Smith, R. C., & Karl, D. M. (2004). Processes regulating oxygen and carbon dioxide in the surface waters of the West Antarctic Peninsula. *Marine Chemistry*, *84*, 161–179.

Dickson, A. G., Sabine, C. L., & Christian, J. R. (Eds.), (2007). (Vol. 3). Guide to best practices for ocean CO₂ measurement. PICES Special Publication.

Eyring, V., Bony, S., Meehl, G. A., Senior, C. A., Stevens, B., Stouffer, R. J., & Taylor, K. E. (2016). Overview of the coupled model intercomparison project phase 6 (CMIP6) experimental design and organization. *Geoscientific Model Development*, *9*(5), 1937–1958. https://doi.org/10.5194/gmd-9-1937-2016

Fay, A. R., Lovenduski, N. S., McKinley, G. A., Munro, D. R., Sweeney, C., Gray, A. R., et al. (2018). Utilizing the Drake Passage Time-series to understand variability and change in subpolar Southern Ocean pCO₂. *Biogeosciences*, *15*(12), 3841–3855. https://doi.org/10.5194/bg-15-3841-2018

Frölicher, T. L., Sarmiento, J. L., Paynter, D. J., Dunne, J. P., Krasting, J. P., & Winton, M. (2015). Dominance of the Southern Ocean in anthropogenic carbon and heat uptake in CMIP5 models. *Journal of Climate*, *28*(2), 862–886. https://doi.org/10.1175/JCLI-D-14-00117.1

Gibson, J. A. E., & Trull, T. W. (1999). Annual cycle of fCO$_2$ under sea-ice and in open water in Prydz Bay, East Antarctica. *Marine Chemistry*, *66*(3-4), 187–200. https://doi.org/10.1016/s0304-4203(99)00040-7

Gray, A. R., Johnson, K. S., Bushinsky, S. M., Riser, S. C., Russell, J. L., Talley, L. D., et al. (2018). Autonomous biogeochemical floats detect significant carbon dioxide outgassing in the high-latitude Southern Ocean. *Geophysical Research Letters*, *45*, 9049–9057. https://doi.org/10.1029/2018GL078013

Gruber, N., Gloor, M., Mikaloff Fletcher, S. E., Doney, S. C., Dutkiewicz, S., Follows, M. J., et al. (2009). Oceanic sources, sinks, and transport of atmospheric CO$_2$. *Global Biogeochemical Cycles*, *23*. https://doi.org/10.1029/2008GB003349

Hauri, C., Doney, S. C., Takahashi, T., Erickson, M., Jiang, G., & Ducklow, H. W. (2015). Two decades of inorganic carbon dynamics along the west Antarctic Peninsula. *Biogeosciences*, *12*(22), 6761–6779. https://doi.org/10.5194/bg-12-6761-2015

Kalnay, E., Kanamitsu, M., Kistler, R., COllins, W., Deaven, D., Gandin, L., et al. (1996). The NCEP/NCAR 40-year reanalysis project. *Bulletin of the American Meteorological Society*, *77*, 437–471. https://doi.org/10.1175/1520-0477(1996)077<0437:tnyrp>2.0.co;2

Khatiwala, S., Tanhua, T., Mikaloff Fletcher, S., Gerber, M., Doney, S. C., Graven, H. D., et al. (2013). Global ocean storage of anthropogenic carbon. *Biogeosciences*, *10*, 2169–2191. https://doi.org/10.5194/bg-10-2169-2013

Landschützer, P., Gruber, N., Bakker, D. C. E., Schuster, U., Nakaoka, S., Payne, M. R., et al. (2013). A neural network-based estimate of the seasonal to inter-annual variability of the Atlantic Ocean carbon sink. *Biogeosciences*, *10*(11), 7793–7815. https://doi.org/10.5194/bg-10-7793-2013

Legge, O. J., Bakker, D. C. E., Johnson, M. T., Meredith, M. P., Venables, H. J., Brown, P. J., & Lee, G. A. (2015). The seasonal cycle of ocean-atmosphere CO$_2$ flux in Ryder Bay, west Antarctic Peninsula. *Geophysical Research Letters*, *42*(8), 2934–2942. https://doi.org/10.1002/2015GL063796

Legge, O. J., Bakker, D. C. E., Meredith, M. P., Venables, H. J., Brown, P. J., Jones, E. M., & Johnson, M. T. (2017). The seasonal cycle of carbonate system processes in Ryder Bay, West Antarctic Peninsula. *Deep Sea Research Part II: Topical Studies in Oceanography*, *139*, 167–180. https://doi.org/10.1016/j.dsr2.2016.11.006

Lenton, A., Metzl, N., Takahashi, T., Kuchinke, M., Matear, R. J., Roy, T., et al. (2012). The observed evolution of oceanic pCO$_2$ and its drivers over the last two decades. *Global Biogeochemical Cycles*, *26*(2), GB2021. https://doi.org/10.1029/2011gb004095

Lenton, A., Tilbrook, B., Law, R. M., Bakker, D., Doney, S. C., Gruber, N., et al. (2013). Sea-air CO$_2$ fluxes in the Southern Ocean for the period 1990-2009. *Biogeosciences*, *10*(6), 4037–4054. https://doi.org/10.5194/bg-10-4037-2013

Loose, B., McGillis, W. R., Schlosser, P., Perovich, D., & Takahashi, T. (2009). Effects of freezing, growth, and ice cover on gas transport processes in laboratory seawater experiments. *Geophysical Research Letters*, *36*(5), L05603. https://doi.org/10.1029/2008GL036318

Lueker, T. J., Dickson, A. G., & Keeling, C. D. (2000). Ocean pCO$_2$ calculated from dissolved inorganic carbon, alkalinity, and equations for K1 and K2: Validation based on laboratory measurements of CO$_2$ in gas and seawater at equilibrium. *Marine Chemistry*, *70*, 105–119. https://doi.org/10.1016/s0304-4203(00)00022-0

Martinson, D. G., & McKee, D. C. (2012). Transport of warm upper circumpolar deep water onto the Western Antarctic Peninsula continental shelf. *Ocean Science*, *8*, 433–442. https://doi.org/10.5194/os-8-433-2012

Martinson, D. G., Stammerjohn, S. E., Iannuzzi, R. A., Smith, R. C., & Vernet, M. (2008). Western Antarctic Peninsula physical oceanography and spatio-temporal variability. *Deep Sea Research Part II: Topical Studies in Oceanography*, *55*, 1964–1987. https://doi.org/10.1016/j.dsr2.2008.04.038

Martz, T. R., Connery, J. G., & Johnson, K. S. (2010). Testing the Honeywell Durafet for seawater pH applications. *Limnology and Oceanography: Methods*, *8*(5), 172–184. https://doi.org/10.4319/lom.2010.8.172

Massom, R. A., & Stammerjohn, S. E. (2010). Antarctic sea ice change and variability - Physical and ecological implications. *Polar Science*, *4*(2), 149–186. https://doi.org/10.1016/j.polar.2010.05.001

Meier, W. N., Fetterer, F., Savoie, M., Mallory, S., Duerr, R., & Stroeve, J. (2017). *NOAA/NSIDC Climate Data Record of Passive Microwave Sea Ice Concentration, Version 3*. Boulder, Colorado USA. NSIDC: National Snow and Ice Data Center. https://doi.org/10.7265/N59P2ZTG

Meredith, M. P., Stammerjohn, S. E., Venables, H. J., Ducklow, H. W., Martinson, D. G., Iannuzzi, R. A., et al. (2017). Changing distributions of sea ice melt and meteoric water west of the Antarctic Peninsula. *Deep Sea Research Part II: Topical Studies in Oceanography*, *139*, 40–57. https://doi.org/10.1016/j.dsr2.2016.04.019

Metzl, N., Brunet, C., Jabaud-Jan, A., Poisson, A., & Schauer, B. (2006). Summer and winter air-sea CO$_2$ fluxes in the Southern Ocean. *Deep Sea Research Part I: Oceanographic Research Papers*, *53*(9), 1548–1563. https://doi.org/10.1016/j.dsr.2006.07.006

Moline, M. A., Karnovsky, N. J., Brown, Z., Divoky, G. J., Frazer, T. K., Jacoby, C. A., et al. (2008). High latitude changes in ice dynamics and their impact on polar marine ecosystems. *Annals of the New York Academy of Sciences*, *1134*, 267–319. https://doi.org/10.1196/annals.1439.010

Montes-Hugo, M., Sweeney, C., Doney, S. C., Ducklow, H., Frouin, R., Martinson, D. G., et al. (2009). Seasonal forcing of summer dissolved inorganic carbon and chlorophyllaon the western shelf of the Antarctic Peninsula. *Journal of Geophysical Research*, *115*(1), C03024. https://doi.org/10.1029/2009JC005267

Moreau, S., Mostajir, B., Bélanger, S., Schloss, I. R., Vancoppenolle, M., Demers, S., & Ferreyra, G. A. (2015). Climate change enhances primary production in the western Antarctic Peninsula. *Global Change Biology*, *21*, 2191–2205. https://doi.org/10.1111/gbc.1287810.1111/gcb.12878

Munro, D. R., Lovenduski, N. S., Stephens, B. B., Newberger, T., Arrigo, K. R., Takahashi, T., et al. (2015). Estimates of net community production in the Southern Ocean determined from time series observations (2002-2011) of nutrients, dissolved inorganic carbon, and surface ocean pCO$_2$ in Drake Passage. *Deep Sea Research Part II: Topical Studies in Oceanography*, *114*, 49–63. https://doi.org/10.1016/j.dsr2.2014.12.014

Munro, D. R., Lovenduski, N. S., Takahashi, T., Stephens, B. B., Newberger, T., & Sweeney, C. (2015). Recent evidence for a strengthening CO$_2$ sink in the Southern Ocean from carbonate system measurements in the Drake Passage (2002–2015). *Geophysical Research Letters*, *42*(18), 7623–7630. https://doi.org/10.1002/2015GL065194

Newberger, T. (2004). *Under way pCO$_2$ System User's Manual, Palmer 2004 pCO$_2$ System Lamont–Doherty Earth Observatory* (p. 23).

O'Neill, B. C., Tebaldi, C., van Vuuren, D. P., Eyring, V., Friedlingstein, P., Hurtt, G., et al (2016). The Scenario Model Intercomparison Project (ScenarioMIP) for CMIP6, *Geoscientific Model Development*, *9*(9), 3461–3482. https://doi.org/10.5194/gmd-9-3461-2016

Orsi, A. H., Whitworth, T., & Nowlin, W. D. (1995). On the meridional extent and fronts of the Antarctic Circumpolar Current. *Deep Sea Research Part I: Oceanographic Research Papers*, *42*, 641–673. https://doi.org/10.1016/0967-0637(95)00021-w

Peng, G., Meier, W. N., Scott, D. J., & Savoie, M. H. (2013). A long-term and reproducible passive microwave sea ice concentration data record for climate studies and monitoring. *Earth System Science Data*, *5*, 311–318. https://doi.org/10.5194/essd-5-311-2013

Resplandy, L., Séférian, R., & Bopp, L. (2015). Natural variability of CO_2 and O_2 fluxes: What can we learn from centuries-long climate models simulations? *Journal of Geophysical Research: Oceans*, *120*(1), 384–404. https://doi.org/10.1002/2014JC010463

Roden, N. P., Shadwick, E. H., Tilbrook, B., & Trull, T. W. (2013). Annual cycle of carbonate chemistry and decadal change in coastal Prydz Bay, East Antarctica. *Marine Chemistry*, *155*, 135–147. https://doi.org/10.1016/j.marchem.2013.06.006

Sabine, C. L., Feely, R. A., Gruber, N., Key, R. M., Lee, K., Bullister, J. L., & Rios, A. F. (2004). The oceanic sink for anthropogenic CO_2. *Science*, *305*(5682), 367–371. https://doi.org/10.1126/science.1097403

Shadwick, E. H. & De Meo, O. A. (2020). CO_2-system observations from a mooring on the West Antarctic Peninsula continental shelf William & Mary. https://doi.org/10.25773/0nxb-wm54

Shadwick, E. H., Thomas, H., Chierici, M., Else, B., Fransson, A., Michel, C., et al. (2011). Seasonal variability of the inorganic carbon system in the Amundsen Gulf region of the Southeastern Beaufort Sea. *Limnology & Oceanography*, *56*(1), 303–322. https://doi.org/10.4319/lo.2011.56.1.0303

Shadwick, E. H., Trull, T. W., Thomas, H., & Gibson, J. A. E. (2013). Vulnerability of polar oceans to anthropogenic acidification: Comparison of Arctic and Antarctic seasonal cycles. *Scientific Reports*, *3*(1), 2339. http://doi.org/10.1038/srep02339

Smith, R. C., Fraser, W. R., Stammerjohn, S. E., & Vernet, M. (2003). Palmer long-term ecological research on the Antarctic marine ecosystem. In E. W. Domack, A. Leventer, A. Burnett, R. Bindschadler, P. Convey, & M. Kirby (Eds.), *Antarctic Peninsula climate variability: Historical and paleoenvironmental perspectives*. American Geophysical Union.

Smith, R. C., Martinson, D. G., Stammerjohn, S. E., Iannuzzi, R. A., & Ireson, K. (2008). Bellingshausen and western Antarctic Peninsula region: Pigment biomass and sea-ice spatial/temporal distributions and interannual variabilty. *Deep Sea Research Part II: Topical Studies in Oceanography*, *55*(18–19), 1949–1963. https://doi.org/10.1016/j.dsr2.2008.04.027

Stammerjohn, S. E., Martinson, D. G., Smith, R. C., & Iannuzzi, R. A. (2008). Sea ice in the western Antarctic Peninsula region: Spatio-temporal variability from ecological and climate change perspectives. *Deep Sea Research Part II: Topical Studies in Oceanography*, *55*, 2041–2058. https://doi.org/10.1016/j.dsr2.2008.04.026

Takahashi, T., Sutherland, S. C., Chipman, D. W., Goddard, J. G., Ho, C., Newberger, T., et al. (2014). Climatological distributions of pH, pCO_2, total CO_2, alkalinity, and CaCO3 saturation in the global surface ocean, and temporal changes at selected locations. *Marine Chemistry*, *164*, 95–125. https://doi.org/10.1016/j.marchem.2014.06.004

Takahashi, T., Sutherland, S. C., Wanninkhof, R., Sweeney, C., Feely, R. A., Chipman, D. W., et al. (2009). Climatological mean and decadal change in surface ocean pCO_2, and net sea–air CO_2 flux over the global oceans. *Deep Sea Research Part II: Topical Studies in Oceanography*, *56*(8-10), 554–577. https://doi.org/10.1016/j.dsr2.2008.12.009

van Heuven, S., Pierrot, D., Rae, J. W. B., Lewis, E., & Wallace, D. W. (2011). Matlab program developed for CO_2 system calculations. Tech. Rep.). ORNL/CDIAC. https://doi.org/10.3334/cdiac/otg.co2sys_matlab_v1.1

Venables, H. J., & Meredith, M. P. (2014). Feedbacks between ice cover, ocean stratification, and heat content in Ryder Bay, western Antarctic Peninsula. *Journal of Geophysical Research: Oceans*, *119*(8), 5323–5336. https://doi.org/10.1002/2013JC009669

Wanninkhof, R. (2014). Relationship between wind speed and gas exchange over the ocean revisited. *Limnology and Oceanography: Methods*, *12*(6), 351–362. https://doi.org/10.4319/lom.2014.12.351

Weeding, B., & Trull, T. W. (2014). Hourly oxygen and total gas tension measurements at the Southern Ocean time series site reveal winter ventilation and spring net community production. *Journal of Geophysical Reserch: Oceans*, *119*(1), 348–358. https://doi.org/10.1002/2013JC009302

Weiss, R. F. (1974). Carbon dioxide in water and seawater: The solubility of a non-ideal gas. *Marine Chemistry*, *2*(3), 203–215. https://doi.org/10.1016/0304-4203(74)90015-2

Williams, N. L., Juranek, L. W., Feely, R. A., Johnson, K. S., Sarmiento, J. L., Talley, L. D., et al. (2017). Calculating surface ocean pCO_2 from biogeochemical Argo floats equipped with pH: An uncertainty analysis. *Global Biogeochemical Cycles*, *31*(3), 591–604. https://doi.org/10.1002/2016gb005541

Williams, N. L., Juranek, L. W., Feely, R. A., Russell, J. L., Johnson, K. S., & Hales, B. (2018). Assessment of the carbonate chemistry seasonal cycles in the Southern Ocean from persistent observational platforms. *Journal of Geophysical Reserch: Oceans*, *123*(7), 4833–4852. https://doi.org/10.1029/2017JC012917

Yang, B., Shadwick, E. H., Schultz, C., & Doney, S. C. (2021). Annual mixed layer carbon budget for the West Antarctic peninsula continental shelf: Insights from year-round mooring measurements. *Journal of Geophysical Reserch: Oceans*, *126*(4), e2020JC016920. https://doi.org/10.1029/2020JC016920